Analysis of 3D printed 17-4 PH stainless steel lattice structures with radially oriented cells

PS. Ginestra, L. Riva, G. Allegri, L. Giorleo, A. Attanasio & E. Ceretti

Department of Mechanical and Industrial Engineering, University of Brescia, Via Branze 38, 25123 Brescia, Italy

ABSTRACT: Additive Manufacturing was initially born as a way to rapid prototyping but the potential of this process made it spread really fast as a production technique. Among all the materials, polymers are the most used for 3D printing but metals are expected to have the biggest growth rate: 38% by 2020. The interest on lattice geometries is widely increasing mainly due to the possibility of obtaining light-weight, well performing and multifunctional products for different fields of application like aerospace, automotive and biomedical. In this work, 17-4PH stainless steel lattice samples with different geometry of cells were manufactured by Selective Laser Melting and tested under uniaxial compression tests. In particular, both the orientation of the cells in relation to the sample and the building orientation of the structures with respect to the building plate were analyzed.

1 INTRODUCTION

Additive Manufacturing (AM) of pure metals can be divided in different sub-categories according with the material charging method: powder bed fusion systems, where materials are added layer-by-layer and direct energy deposition systems, where materials are added through a nozzle or a wire fed system (Lowther et al. 2019). Cellular structures are usually divided in two major groups: stochastic porous structures and cellular lattice structures (Yan et al. 2014). Stochastic porous structures are characterized by pores located randomly throughout the entire volume of the object, thus, the mechanical properties result not uniform and difficult to control. Cellular lattice structures consist in a unit cell repeated in all directions, making the mechanical properties controllable and repeatable. Consequently, lattice structures with a certain volume fraction present better mechanical properties than stochastic porous structures. As an example, in the aerospace field, the production of a component with the same level of performances but a reduced weight consists in a huge economical advantage. On the biomedical side, lattice structures can be advantageous enhancing the properties of implanted prostheses and functional orthoses (Ginestra et al. 2016). Moreover, the surface properties of a metal lattice structure can improve the interaction with the physiological environment by stimulating cells through their morphology which was found to be a key factor for the biointegration of a scaffold (Gastaldi et al. 2015, Ginestra et al. 2017a,b). Furthermore, an open cell structure makes a sample suitable even for non-structural application like acoustic insulation, energy absorption and filtration.

Selective Laser Melting (SLM) of lattice structures is a relatively new process so there is no complete characterization of their performances in the literature yet. The properties of the lattice structures depend on several factors: cell geometry, material, struts dimension, loading directions and boundary conditions (Leary et al. 2018). Although the lattice structures have a lot of advantageous properties there are some issues that have to be taken into account. The majority of the possible geometries is not isotropic, consequently the mechanical properties of an object show an anisotropic trend. Moreover, only few materials and geometries have been studied and the comparison between different results is often difficult due to the differences in tests procedures, process parameters and printing quality (Marbury 2017).

For example, the orientation of the cells within the sample changes the number of struts in the direction of compression causing a change in the strength of the sample. It also changes the thermal gradient that the part is subjected to, and consequently also the residual stresses within the structure. The study of different orientations is then fundamental for a complete analysis of the potential of lattice geometries. Moreover, considering the widespread use of lattice structures for load-bearing prostheses design in the biomedical field, a radial orientation of the cells within a lattice sample would replicate the structure of the Harvesian lamellae of the cortical bone (Rho et al. 1998). In this work, 17-4 PH Stainless Steel was used to manufacture cylindrical lattice samples via SLM. The high tensile stress and hardness combined with a good corrosion resistance below 315°C make this material appealing for many applications (Mahmoudi et al. 2017). The geometry of three different cells was chosen considering the most representative unit cells for cellular lattices available in the majority of the printers' design platforms and currently analyzed in literature (Jin et al. 2019, Maskery et al. 2018). The building orientation of the samples was modified to evaluate the effect of these parameters on the mechanical performances of the structures.

2 MATERIALS AND METHODS

17-4PH stainless steel powder was used as printing material. All the powders were selected from the same batch to exclude the influence of the material. The powder exhibits spherical shape particles with a size in the range of 5-35 µm (Zhang et al. 2017). The chemical composition is reported in Table 1.

Table 1. Chemical composition of 17-4PH stainless steel powder.

17-4 PH	Cr	Ni	Cu	Mn	Mo	Nb	Si
Wt (%)	16.71	4.09	4.18	0.8	0.19	0.23	0.53

The low content of impurities is crucial to avoid side effects of embrittlement. The samples were manufactured using a laser based powder bed fusion machine (ProX 100, 3D SYSTEMS). The laser melting process occurred in a protective Nitrogen atmosphere with O_2 content less than 0.1 vol.% and the processing parameters were set as reported in Table 2. Three replicas of each produced substrate have been analyzed for the compression tests. When the SLM process was finished, the samples were removed from the plate through a band saw.

Table 2. Process parameters used in the SLM process.

Process Parameter	Value
Laser power (W)	50
Spot diameter (µm)	80
Scan speed (mm/s)	300
Hatch spacing (µm)	50
Layer thickness (µm)	30

2.1 *Design and production of the lattice structures*

The lattice structures studied in this paper were generated by means of the integrated software 3DXpert. In particular, three different geometries were selected: diagonal, diamond and face centric cubic cells (FCC) (Fig. 1).

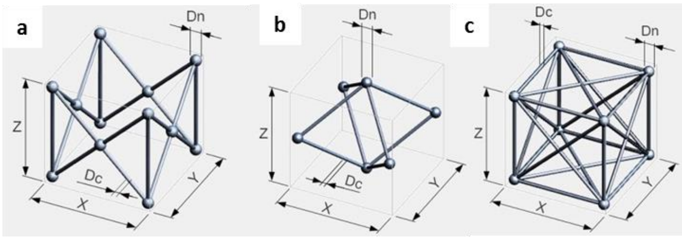

Figure 1. Diagonal (a), Diamond (b) and FCC (c) unit cells.

The dimensions of the unit cells were kept to 2(X) x 2(Y) x 2(Z) mm^3. A diameter of struts (Dc) of 0,5 mm and spherical nodes (Dn) of 1 mm were selected. Following the ISO standard 13314, cylindrical samples with a 24 mm diameter and a 30 mm height were produced. Two building orientations were considered: 0° and 90° in relation to the building plate direction (Fig. 2).

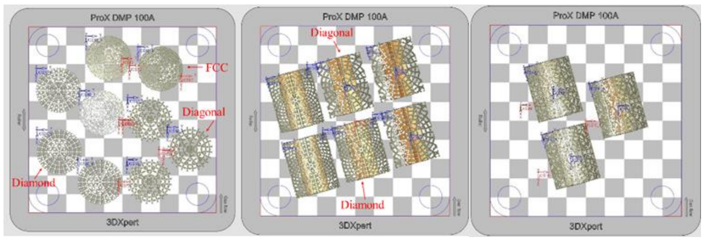

Figure 2. Building plates design in 3DXpert. The direction of the roller is up-down.

In order to analyze the effect of the cells orientation on the mechanical properties of the samples, the cells were arranged with a radial distribution, in which the cells are not lined up one next to the other but form concentric features (Fig. 3).

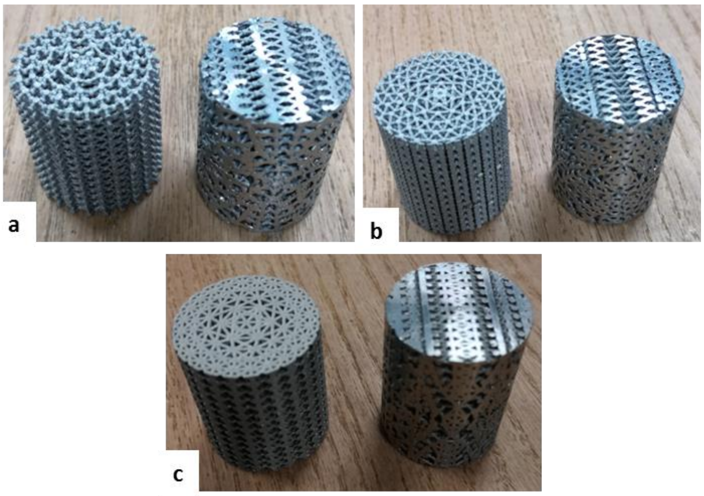

Figure 3. Samples manufactured with 0° (left) and 90° (right) building orientation: Diagonal (a), Diamond (b) and FCC (c).

2.2 *Characterization of the lattice samples*

In order to obtain the relative density of the samples, the geometry and weight of the lattices were analyzed. The height and diameter of the cylinders were measured with a digital caliber while a microbalance was used to obtain the weight and calculate the relative density of the samples. The surface morphology of the samples was observed under an Hirox RH-2000 optical microscope.

The mechanical response of the lattice samples was evaluated by uniaxial compression tests carried out at 23° C by means of a hydraulic press equipped with a 1000kN load cell. The specimens were subjected to a compressive ramp under force control up to a displacement of 15 mm without intermittence. The samples oriented at 0° were subjected to a load parallel to the building direction while the samples built at 90° were subjected to a load perpendicular to the building direction. The results are reported as nominal stress vs. nominal strain curves, where the nominal stress is the force normalized on the overall specimen cross-section (about 452 mm^2), while the nominal strain is the crosshead displacement normalized on the overall specimen thickness (Ceretti et al. 2017). This representation allowed an easier comparison of the various structures, avoiding effects ascribed to the differences in the cross-section of the samples. The elastic modulus (E) was considered as the slope of the linear fit of the stress-strain curve.

3 RESULTS

3.1 *Morphology of the samples*

The geometry of the samples was analyzed to evaluate the comparison between the designed models and the as-built samples and revealed a good consistency of the production process (Table 3).

Table 3. Geometry data of the as built samples.

Sample	Building angle (°)	Diameter (mm)	Height (mm)
Diagonal	0	23.8±0.06	29.4±0.07
	90	23.4±0.01	30.0±0.05
Diamond	0	24.1±0.04	29.4±0.06
	90	23.4±0.02	30.0±0.01
FCC	0	24.1±0.06	29.5±0.02
	90	23.8±0.01	29.9±0.01

The higher dispersion of data in relation to the diagonal cells is due to the geometry of the samples that may influence the right positioning of the caliber. As for the other cells geometries, the slightly higher standard deviation on the diameter of the samples built at 0° is probably due to the cutting edges. The relative density was analyzed considering that the volume fraction is one of the key parameters controlling the mechanical properties of porous parts (Table 4).

Table 4. Weight and density values calculated on the as built samples.

Sample	Building angle (°)	Weight (g)	Relative density (g/mm^3)
Diagonal	0	27.3±0.37	2.1E-03
	90	29.6±0.04	2.3E-03
Diamond	0	30.0±0.07	2.2E-03
	90	29.5±0.16	2.3E-03
FCC	0	39.5±1.97	3.0E-03
	90	44.0±1.19	3.3E-03

The building orientation of the samples has a reduced impact on the relative density of the parts while the geometry of the cells, especially for the FCC configuration, may cause the presence of unmelted powder trapped inside the structure causing an increase of the relative density.

The surface morphology of the produced samples was observed to identify the presence of defects and collapsed struts (Fig. 4).

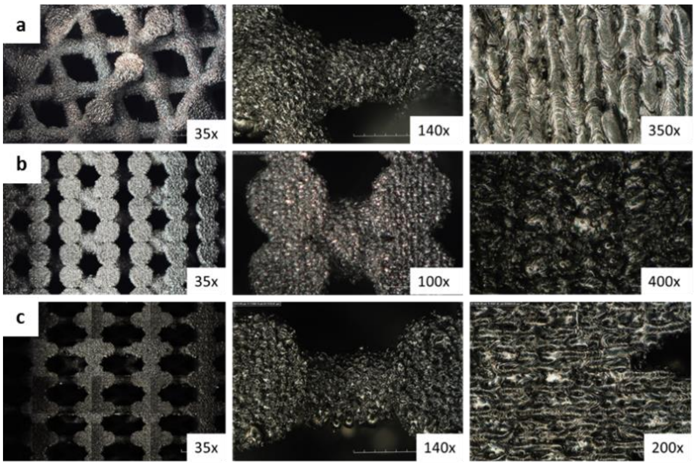

Figure 4. Optical microscope images at different magnifications of the samples manufactured with 0° building orientation: Diagonal (a), Diamond (b) and FCC (c).

The struts and the nodes show the typical cylindrical and spherical shapes but their surfaces are covered with partially melted powder on the top layer.

At higher magnifications (Fig. 4), it is possible to see the path followed by the laser while scanning and melting the powder.

3.2 *Mechanical response*

The results of the compression tests are reported in terms of the nominal stress (i.e. stress over the initial section) vs. the engineering strain (i.e. the displacement over the overall specimen thickness) and are compared in Figures 5 and 6, as the most representative nominal stress vs. nominal strain curves for each material group. In this representation, the use of normalized force versus displacement allows the comparison between specimens with different cross sections and thickness.

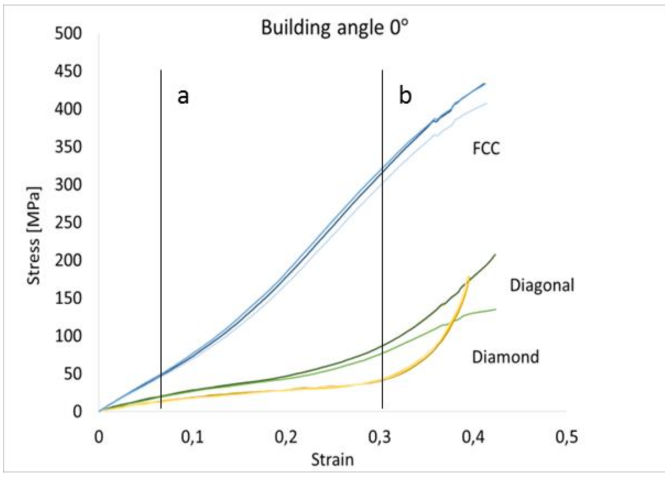

Figure 5. Nominal stress vs. nominal strain curves obtained from the compression tests performed on the samples built at 0° of orientation.

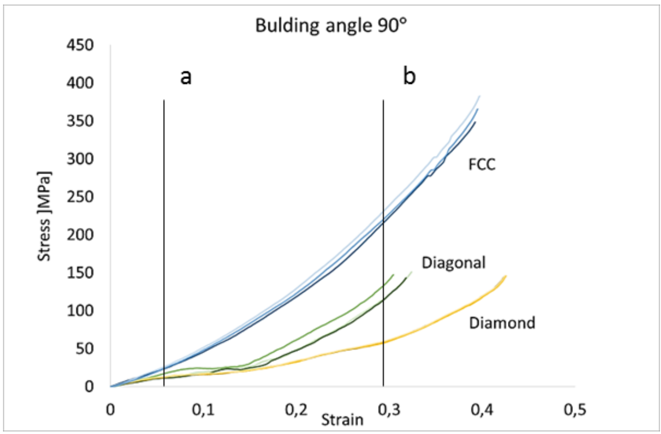

Figure 6. Nominal stress vs. nominal strain curves obtained from the compression tests performed on the samples built at 90° of orientation.

All the curves show the occurrence of a multi stage compression history, as suggested by the three different slopes of the curves: the early deformation of the structure allows to evaluate the material stiffness at small strains (Fig. 7). This trend is followed by a reduction of the slope as a possible consequence of the collapse of the structure trough local collapses of the lattice layers. Finally, a subsequent increase of the slope is found after the collapsed structure has approached a more compact state. In particular, the early elastic deformation stage is followed by a plastic deformation region at higher values of strain (Fig. 5 and 6 line a), a subsequent collapse stage and a final hardening stage (Fig. 5 and 6 line b).

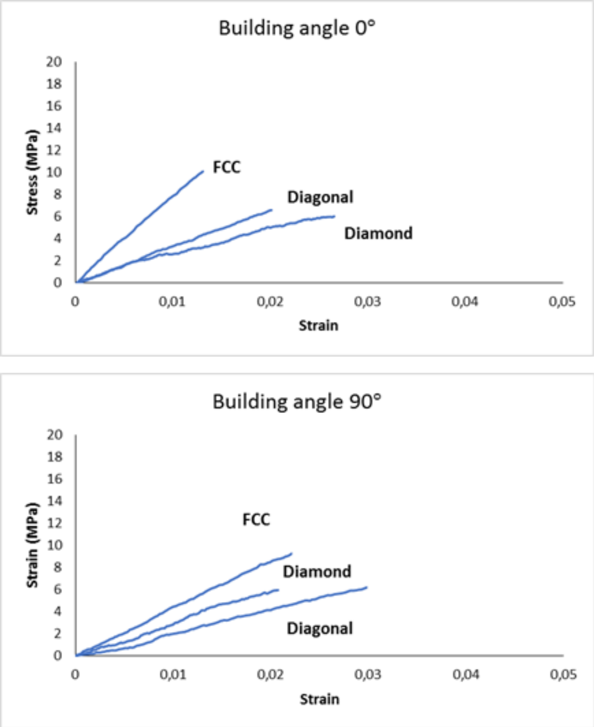

Figure 7. Detail of the early elastic deformation stage on the samples built at 0° and 90° of orientation.

The difference in the performances between the two orientations for the diagonal and FCC samples are probably caused by an anisotropy due to different number of struts in the direction of the compression, especially for the FCC configuration. In particular, the obtained curves for the samples oriented at 90° are influenced by an effect of densification of the structure that requires higher levels of stress compared to the other cells geometries. As for the diamond geometry, it can be observed that the building direction is not affecting the mechanical response in the same way, leading to a more isotropic behavior of these cells highlighted by the evident replicability of the compression trend. With regard to the diagonal geometry, the difference found between the trends observed at different building orientations is probably due to the less presence of struts parallel to the compression direction. The nominal stress vs. nominal strain curve stiffness (i.e. the slope of the curve in the linear initial trend) is reported in Table 5.

Table 5. Stiffness (E) calculated on the samples tested under compression.

Sample	Building angle (°)	E (MPa)
Diagonal	0	391.1±51.9
	90	261.9±36.1
Diamond	0	225.8±33.3
	90	286.0±29.3
FCC	0	782.5±35.6
	90	416.0±23.3

The reason of the observed difference between the stiffness calculated for the FCC configuration at different building orientations is probably the radial distribution of the cells that caused the two orientations to have very distinct internal structures and therefore different mechanical properties compared to the typical isotropic behavior of these cells.

The compressed samples are shown in Figure 8.

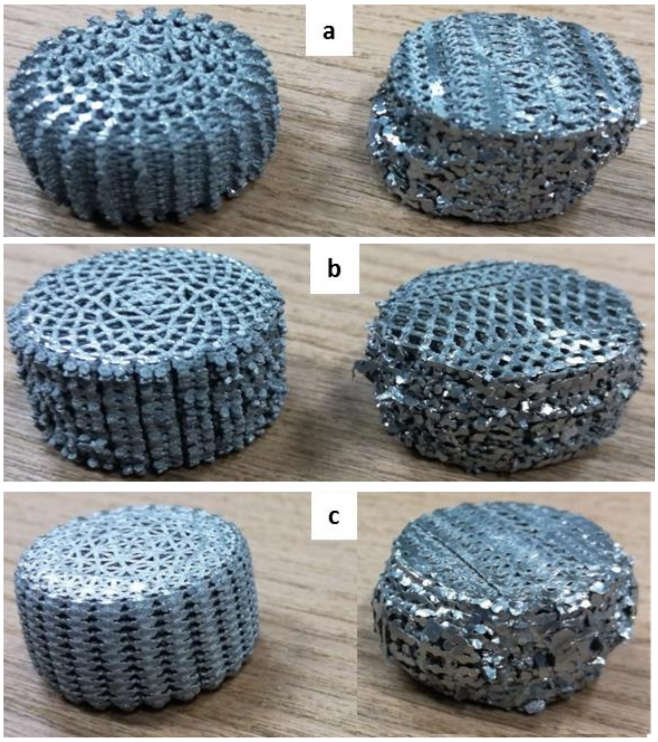

Figure 8. Compressed samples: Diagonal (a), Diamond (b) and FCC (c).

The images of the compressed samples show the layer-by-layer buckling deformation, typical of the lattice structures, that was accompanied by a shear band (45°) clearly visible for the diagonal configuration as already observed for this type of geometry (Liu et al. 2018).

4 CONCLUSION

In this work, 17-4PH stainless steel lattice cylinders with a radial distribution of cells were built using a 3D printer. Three cell geometries, diagonal, diamond and FCC, and two different building orientations, 0° and 90°, were chosen. The 3DXpert software was used to design the samples, produced using the ProX100 printer (3D SYSTEMS). The structures were characterized and subjected to compression tests by means of an hydraulic press. The geometry of the designed samples was reproduced by the process with an error of less than 1% and the geometries of the struts and nodes have been produced without defects. Regarding the mechanical performances of the samples under compression tests, the results suggested that when a diagonal geometry of the cells is used, the building orientation can strongly influence the mechanical properties. In particular, the stiffness of the samples is higher in relation to a building orientation of 0° probably due to the higher number of struts along the compression direction. The diamond geometry showed isotropic mechanical properties almost independent from the building orientation of the structures. As for the FCC cells, the stiffness of the samples calculated in correspondence to a building orientation of 0° was significantly higher than the value calculated for the samples built at 90° with respect to the building plate. Although the geometry of the cells is isotropic, the performances resulted very different. Considering the relationship between the volume fraction and the mechanical properties of these samples, the results suggest that the radial orientation of the cells can influence the mechanical response of the lattice structures when the geometry of the cells can be varied by giving a radial distribution in relation to the building orientation.

The anisotropy of the mechanical properties found in SLM parts can be attributed to the oriented layer-by-layer growth process along the direction of the substrate. As expected, an increase of the overall system stiffness is found as the density increases. This suggests the possibility to easily tune the stiffness of the lattices, and to vary the object structure without significant changes in the overall stiffness. In particular, the optimization of the orientation of the cells can improve the mechanical properties of the lattice structures and enhance the performance efficiency of the produced cellular parts and, as a consequence, enhance the performances of the final product.

5 REFERENCES

Ceretti, E., Ginestra, P., Neto, P.I., Fiorentino, A., Da Silva, J.V.L. 2017. Multi-layered scaffolds production via Fused Deposition Modeling (FDM) using an open source 3D printer: process parameters optimization for dimensional accuracy and design reproducibility. *Proedia. CIRP* 65: 13-18.

Gastaldi, D., Parisi, G., Lucchini, R. et al. 2015. A Predictive Model for the Elastic Properties of a Collagen-Hydroxyapatite Porous Scaffold for Multi-Layer Osteochondral Substitutes, *International Journal of Applied Mechanics* 7(4): 1550063.

Ginestra, P.S., Ceretti, E., Fiorentino, A.2016. Potential of modeling and simulations of bioengineered devices: Endoprostheses, prostheses and orthoses. *Proceedings of the Institution of Mechanical Engineers, Part H: Journal of Engineering in Medicine* 230(7): 607-638.

Ginestra, P., Fiorentino, A., Ceretti, E. 2017. Micro-structuring of titanium collectors by laser ablation technique: a novel approach to produce micro-patterned scaffolds for tissue engineering applications. *Procedia CIRP* 65:19-24.

Ginestra, P.S., Pandini, S., Fiorentino, A. et al. 2017. Micro-structured scaffold for guided cellular orientation: Poly(ε-caprolactone) electrospinning on laser ablated titanium collector. *CIRP Journal of Manufacturing Science and Technology* 19:147-157.

Jin, N., Wang, F., Wang, Y., et al. 2019. Failure and energy absorption characteristics of four lattice structures under dynamic loading, *Materials and design* 169:107655.

Leary, M., Mazur, M., Williams, H., et al. 2018. Inconel 625 lattice structures manufactured by selective laser melting (SLM): Mechanical properties, deformation and failure modes. *Materials and design* 157:179-199.

Liu, F., Zhang, D.Z., Zhang, P., Zhao, M., Salman J. 2018. Mechanical Properties of Optimized Diamond Lattice Structure for Bone Scaffolds Fabricated via Selective Laser Melting *Materials* 11:374. doi:10.3390/ma11030374.

Lowther, M., Louth, S., Davey, A. et al., 2019. Clinical, industrial, and research perspectives on powder bed fusion additively manufactured metal implants, *Additive Manufacturing* 28:565-584.

Mahmoudi, M., Elwany, A., Yadollahi, A. et al., 2017. Mechanical properties and microstructural characterization of selective laser melted 17-4 PH stainless steel, *Rapid Prototyping Journal* 23:280-294.

Maskery, I., Sturm, L., Aremu, A.O., et al. 2018. Insights into the mechanical properties of several triply periodic minimal surface lattice structures made by polymer additive manufacturing, *Polymer* 152: 62-71.

Marbury, F., 2017. Characterization of SLM Printed 316L Stainless Steel and Investigation of Micro Lattice Geometry. PhD dissertation.

Rho, J.Y., Kuhn-Spearing, L., Zioupos, P., 1998. Mechanical properties and the hierarchical structure of bone, *Medical Engineering and Physics* 20: 92-102.

Yan, C., Hao, L., Hussein, A., et al. 2014. Advanced lightweight 316L stainless steel cellular lattice structures fabricated via selective laser melting, *Materials and Design*, 2014 55: 533-541.

Zhang, Z., Peng, T., Xu, S. 2017. The influence of scanning pattern on the part properties in powder bed fusion processes: an experimental study. *Procedia CIRP* 61: 606-611.